

this alloy at ultralow temperatures jointly with a Czechoslovakian research group by the method of thermocycling of oriented nuclei on the "spin" setup at the Laboratory of Nuclear Studies at the Joint Institute for Nuclear Research (Dubna).⁷ It should be emphasized that the characteristic time of the experiment in the method of the Mössbauer effect on oriented nuclei, which we employed, is determined both by the lifetime of the excited state of the nucleus ($\sim 10^{-7}$ s) and the nuclear spin-lattice relaxation time, which significantly extends the range of relaxation frequencies accessible to observation.

The distribution functions of the molecular fields at different temperatures, showing that the spontaneous magnetization of the alloy is described well by the percolation model,⁸ were determined for a ferromagnetic alloy with an impurity concentration of 0.15 at. % Fe. Such distribution functions, determining the main magnetic properties, were also obtained for alloys in the paramagnetic phase in applied fields.

2. There now exist data on HF fields on nonmagnetic impurities in Fe, Co, and Ni ferromagnetic matrices for most elements in Mendeleev's table. The theoretical calculations of these fields are in good agreement with experiment (see, for example, Ref. 9). The studies of the HF saturation fields $H_{\text{hf}}(0)$ on the nonmagnetic impurity Sn in a rare-earth metal showed that in different matrices $H_{\text{hf}}(0)$ deviates from the expected linear dependence on the projection of the spin of the rare-earth ion on the total moment $(g-1)J$. Analogous deviations have been observed for other nonmagnetic impurities in other studies. This behavior was also observed in a series of intermetallic compounds of rare earths, which supports the idea that the exchange interaction Hamiltonian does not have a purely spin character (JS_s), but rather contains other interactions also, which take into account orbital motion and the spin-dipole contribution (see, for example, the review of Ref. 10).

It was found that the HF field on Sn as a function of temperature $H_{\text{hf}}(T)$ follows the spontaneous magnetization curve only in the case of a Gd matrix. In other heavy rare-earth metals, as in the case of 3d matrices, large deviations are observed in the behavior of these curves. Based on these "temperature" anomalies in the HF fields we concluded that the spontaneous polarization of the conduction electrons $P = (N_{\uparrow} - N_{\downarrow}) / (N_{\uparrow} + N_{\downarrow})$ inducing an HF field on the impurity, generally speaking, is not proportional to the magnetization $\langle J_z \rangle / J$.¹¹ The absence of such a proportionality should be manifested in cases when near the Fermi level the curves of the distribution of the electronic density of states in subbands with spin \uparrow and \downarrow rapidly change in an energy interval of the order of the magnitude of the exchange splitting.

Existing results of calculations of band structures for pure matrices and for the contributions of electrons with spin \uparrow and \downarrow to the HF field on the impurity agree qualitatively with this assumption.

The magnetic ordering of REM is characterized by a large diversity of magnetic structures, and HFI for the nonmagnetic impurity Sn can be employed to obtain additional information about them. The phenomenon of hysteresis of the HF field, caused by the change produced by the applied field in the magnetic structure which after the field is removed does not return to the starting state because of the existence of a potential barrier, was discovered by this method.

Data confirming the proposition that the nonmagnetic impurity distorts the magnetic structure of the nearest-neighbor environment were obtained.¹² Model numerical calculations performed in Ref. 13 showed that the impurities, regarded as magnetic defects, can create local magnetic structures, the interactions between which can give rise to a new type of magnetic state, which in Ref. 13 was given the name pseudo-spin glass. The existence of such a state has not yet been demonstrated, but the complex Mössbauer spectra observed, for example, for Sn in Dy can be understood by assuming that we are dealing with a system in a pseudo-spin glass state.

¹V. A. Andrianov, M. G. Kozin, A. Yu. Pentin, V. V. Turovtsev, and V. S. Shpinel', Abstracts of Reports at the 23rd All-Union Conference on Low-Temperature Physics (in Russian), Tallin (1984), Part 3, p. 6.

²A. I. Larkin and V. I. Mel'nikov, Zh. Eksp. Teor. Fiz. **61**, 1231 (1971) [Sov. Phys. JETP **34**, 656 (1972)].

³V. A. Andrianov, M. G. Kozin, A. Yu. Pentin, V. V. Turovtsev, and V. S. Shpinel', Zh. Eksp. Teor. Fiz. **85**, 627 (1983) [Sov. Phys. JETP **58**, 364 (1983)].

⁴R. P. Peters, Ch. Buchal, M. Kubota *et al.*, Phys. Rev. Lett. **53**, 1108 (1984).

⁵V. A. Andrianov, M. G. Kozin, A. Yu. Pentin, V. S. Shpinel', and Dao Kim Ngok, Abstracts of Reports at the 24th All-Union Conference on Low-Temperature Physics (in Russian), Tbilisi (1986), Part III, p. 18.

⁶J. Flouquet, O. Taurian, J. Sanchez, M. Chapellier, and J. L. Tholence, Phys. Rev. Lett. **38**, 81 (1977).

⁷J. Englich, B. Lestak, M. Rotter, B. Sedlak, M. Finger, V. N. Pavlov, V. A. Andrianov, M. G. Kozin, and V. S. Shpinel', Hyperfine Interactions **22**, 77 (1985).

⁸I. Ya. Korenblit and E. F. Shender, Usp. Fiz. Nauk **126**, 233 (1978) [Sov. Phys. Usp. **21**, 832 (1978)].

⁹J. Kanamori, H. Akai, and M. Akai, Hyperfine Interactions **17-19**, 287 (1984).

¹⁰V. S. Shpinel', Phys. Status Solidi B **118**, 11 (1983).

¹¹S. I. Reiman, N. I. Rokhlov, V. S. Shpinel', and E. P. Kaminskaya, Zh. Eksp. Teor. Fiz. **86**, 330 (1984) [Sov. Phys. JETP **59**, 190 (1984)].

¹²S. K. Godovikov, V. V. Metlushko, V. S. Shpinel', and A. I. Firov, Abstracts of Reports at the 1st All-Union Conference on Nuclear-Spectroscopic Studies of Hyperfine Interactions (in Russian), M., 1985, p. 44.

¹³M. W. Dunlop and D. Sherrington, J. Phys. C **18**, 1465 (1985).

G. B. Khristiansen. *Apparatus for studying extremely high energy cosmic rays.* The energy spectrum of galactic (and possibly metagalactic) cosmic rays encompasses a colossal energy range from several tens of MeV up to at least 10^{20} eV. Cosmic rays have in recent years been studied espe-

cially intensively by so-called "direct" methods, i.e., by recording and studying the primary cosmic radiation itself (which is possible in practice up to energies of 10^{14} - 10^{15} eV). These studies led to the following picture of the generation and propagation of galactic cosmic rays with energies

up to 10^{13} – 10^{14} eV; a) cosmic rays diffuse in random magnetic fields in the galaxy so that their transport range depends on the energy $\lambda(E_0) \sim E_0^\alpha$; $\alpha = 0.3 - 0.6$ ¹; b) cosmic rays are generated during acceleration by shock waves in the shells of supernovae²; c) the energy spectrum of the cosmic rays generated is very hard, $F(E_0)dE_0 \sim E_0^{-(2+\epsilon)}$ dE_0 ($\epsilon = 0.1 - 0.3$), and corresponds to a compression factor of $\rho_2/\rho_1 = \sigma \approx 4$ (since according to the theory of acceleration $3/(\sigma - 1) = 1 + \epsilon$). The maximum energy of the generated protons is $E_0 \approx 10^{13}$ – 10^{14} eV.

At the same time the experimental data, obtained now not by direct, but rather by indirect methods for recording the primary cosmic rays, indicate the existence of primary particles with energies many orders of magnitude higher than 10^{14} eV. The energy spectrum of cosmic rays studied by these methods, i.e., by recording extensive atmospheric showers (EAS), shows that a) there exists a “break” at an energy of $\sim 3 \cdot 10^{15}$ eV (the index of the primary energy spectrum increases here by 0.5–0.7); b) the intensity of the cosmic rays as a function of their energy drops according to the law $E(>E_0) \sim E_0^{-2}$ in the region 10^{17} eV $< E_0 < 10^{19}$ eV; and, c) the primary radiation contains particles with a minimum energy of several joules. This collection of facts has not yet been convincingly explained quantitatively, though there exists a number of semiquantitative models. The accuracy of the experimental data in the region $E_0 > 10^{15}$ eV is apparently still not high enough to construct a quantitative picture of the generation and propagation of cosmic rays at these energies.

Figure 1 shows the modern data³⁻⁷ on the energy spectrum of the primary cosmic rays in the energy range $E_0 = 10^{15}$ – 10^{20} eV. The existence of a “break” has been established without doubt, and the general behavior of the spectrum up to energies of $\sim 10^{19}$ eV can also be regarded as known approximately. The observed spread in the experimental data, however, especially for $E_0 > 10^{19}$ eV, is very large and precludes the solution of the well-known problem of the “cutoff” of the spectrum owing to the interaction of metagalactic cosmic rays with the relic radiation (G. T. Zatsepin and V. A. Kuz'min⁸). Of course, one can hardly talk about details (for example, irregularities) in the behavior of the spectrum at lower energies (10^{17} – 10^{19} eV) also.

The data on the anisotropy of cosmic rays with energy exceeding 10^{15} eV and especially the data on the nuclear

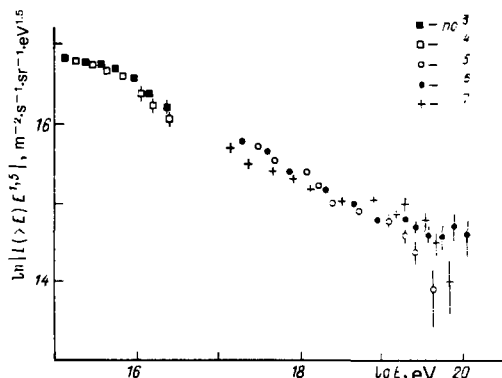


FIG. 1. For $E > 10^{15}$ eV the intensity equals $60 \text{ m}^{-2} \cdot \text{sr}^{-1} \cdot \text{yr}^{-1}$; for $E > 10^{18}$ eV it is $60 \text{ km}^{-2} \cdot \text{sr}^{-1} \cdot \text{yr}^{-1}$, for $E > 10^{19}$ the intensity is $\sim 0.6 \text{ km}^{-2} \cdot \text{sr}^{-1} \cdot \text{yr}^{-1}$.

composition at these energies are even more uncertain. In the latter case different authors even arrive at directly opposite conclusions about the relative role of protons and nuclei with large values of A in the primary cosmic radiation.

After D. V. Skobel'tsyn and G. T. Zatsepin discovered the nuclear-cascade process in EAS, created by cosmic rays with ultrahigh energy ($> 10^{15}$ eV), the method proposed by G. T. Zatsepin for studying the transverse development of individual EAS has been widely used.⁹ This method was used to obtain the results mentioned above as well as to study a number of phenomena accompanying EAS, for example, emission of radio waves, optical radiation (Cherenkov and ionization), etc. The optical radiation flux in this case turned out to be a good measure of the energy of the primary particle created by the EAS (A. E. Chudakov).¹⁰

Comparison of the character of the spatial distribution for the electrons, muons, optical photons, and radio radiation of EAS shows that the spatial distribution of optical photons and the spatial distribution of electrons is wider than the spatial distribution of the coherent radio radiation. Because of the limited time available for optical observations (5–10%) and the small role of muons in the EAS relative to that of electrons ($< 10\%$), electrons in EAS are the component which is most conveniently recorded in any type of weather and requires a smaller sensitive detector area.

Thus in designing new apparatus it is desirable to concentrate on recording primary cosmic rays with energies 10^{15} – 10^{20} eV with the help of primarily the electronic component (or, more accurately, the charged particles) in EAS, employing also its optical radiation.

Studies performed in recent years have shown that particle avalanches do not arrive simultaneously at the plane of observation, but rather with a spread, which increases as the distance from the axis of the EAS increases.¹¹ In addition, it can be shown that the avalanche front is not flat. It is important to take these facts into account in order to determine more accurately the orientation and other parameters of the EAS. The accuracy of the determination of the main parameters of the EAS (the position, zenith angle, and azimuthal angle of the axis and the number of particles) depends

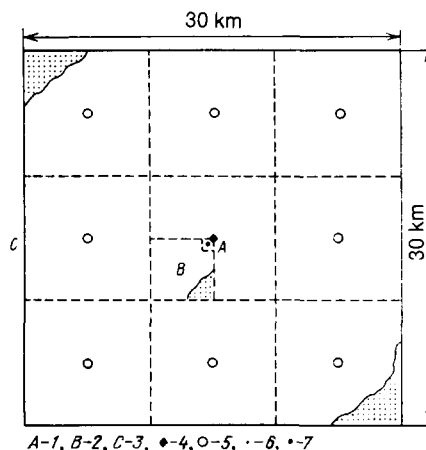


FIG. 2. 1) Territory with an area of 1 km^2 , 2) territory with an area of 25 km^2 , 3) the entire territory (10^3 km^2), 4) central point of detection, 5) reference points for detection, 6) detection points with an area of 1 m^2 , 7) muon detector.

strongly on the number of charged-particle detectors employed in the experimental apparatus.

The basic methodological principle on which the new apparatus near sea level is based is a fundamental (by a factor of 30 to 50) increase, compared with other apparatus, in the density of charged-particle detectors in the territory in which the EAS is recorded. At the same time, just as in the case of apparatus of the preceding generation, the area of the territory increases (and the density of detectors decreases) as the energy of the EAS recorded increases. This principle is illustrated in Fig. 2, which shows the arrangement of the charged-particle detectors. Near the center of the installation, there are about $2.5 \cdot 10^3$ detectors (plastic scintillators with an area of 1 m^2 each) in an area A of size $1 \times 1 \text{ km}^2$. The distance between the detectors is 20 m. This system is used to detect and measure EAS with energies 10^{15} – 10^{17} eV. The territory A is a $5 \times 5 \text{ km}^2$ part of the territory B in which there are about $5 \cdot 10^3$ detectors. This system is used to study EAS with energies of 10^{17} – 10^{19} eV. Finally, the territory C with an area of 10^3 km^2 is covered with about $3.6 \cdot 10^3$ detectors and is used to record EAS with energies of 10^{18} – 10^{20} eV. The significantly higher detector density in this installation, compared with installations of the previous generation, not only improves the accuracy with which the parameters of the EAS are determined, but it also enlarges significantly (by orders of magnitude) the statistical sample of the EAS of different energies (from 10^{15} up to 10^{18} eV) with high efficiency. This is extremely important in order to make an accurate investigation of the anisotropy of ultrahigh energy cosmic rays. It is proposed that the following will also be placed at the center of the entire installation: a) a detector for muons with energies above 1–2 GeV with a total area of 10^3 m^2 ; b) detectors for optical radiation from the EAS in order to record the optical radiation flux both integrated over time and differentiated in time. The latter, as shown in Ref. 12, will give information about the longitudinal development of individual EAS (in particular, the position of the maximum of the electron avalanche). The indications of the muon detector are sensitive to the atomic number A of the primary particle generating the EAS. The combination of data from the large-area muon detector and data on the electronic component and Cherenkov radiation of EAS will make it possible to put the question of the nuclear composition of the cosmic rays at energies of 10^{15} – 10^{18} eV on a quantitative footing (see Ref. 13). Much depends here also on our knowledge of hadron-nucleus and nucleus-nucleus interactions at ultrahigh energies. Investigations using accelerators over the years in which the proposed installation is to be developed will apparently make it possible to clarify this question. The relative calibration of the “direct” and “indi-

rect” methods will also play a large role here.

Thus the planned apparatus will make it possible to determine the following with the help of “indirect” methods for recording cosmic rays with energies of 10^{15} – 10^{20} eV: 1) the energy spectrum and the absolute flux of cosmic rays in the indicated energy range (and in addition new irregularities in the spectrum, if they exist, will be revealed and the question of the “relic cutoff” of the spectrum will be solved; 2) the anisotropy of cosmic rays with energy 10^{15} – 10^{20} eV using a statistical sample which is tens and hundreds of times larger than the sample previously available to experimentalists; 3) new data on the nuclear composition of primary radiation with energy 10^{15} – 10^{18} eV on a higher quantitative level; 4) proof of the existence of sources of ultrahigh energy gamma rays, if their flux indeed corresponds to the preliminary data from the Kiel group; and, 5) experimental data on the longitudinal and transverse development of EAS in order to check the applicability of different models of hadron-nucleus and nucleus-nucleus interactions at ultrahigh energies up to 10^{20} eV.

We note that the proposed installation can also be used to solve a number of problems related with the study of the heliosphere and the earth’s magnetosphere by studying the variations of the cosmic-ray intensity. This possibility is provided by the large total detector area in the planned installation.

- ¹J. J. Engelman, P. Goret *et al.*, *Astron. Astrophys.* **148**, 12 (1985).
- ²G. F. Krymskiĭ, A. I. Kuz’min *et al.*, *Proceedings of International Cosmic Ray Conference* (1979), Vol. 2, pp. 39, 44.
- ³Yu. A. Fomin and G. B. Khristiansen, *Proceedings of the 7th European Symposium on Cosmic Rays*, Leningrad Institute of Nuclear Physics, USSR Academy of Sciences, L., 1980, p. 77.
- ⁴T. A. Alimov, Author’s Abstract of Candidate’s Dissertation (in Russian), L., 1985.
- ⁵M. I. Pravdin, Author’s Abstract of Candidate Dissertation (in Russian), M., 1985.
- ⁶A. J. Bower *et al.*, *Proceedings of International Cosmic Ray Conference, Bangalore* (1983), Vol. 9, p. 207.
- ⁷R. M. Baltrusaitis, R. Cady, G. L. Cassidy *et al.*, *Phys. Rev. Lett.* **54**, 1875 (1985).
- ⁸G. T. Zatsepina and V. A. Kuz’min, *Pis’ma Zh. Eksp. Teor. Fiz.* **4**, 114 (1966) [*JETP Lett.* **4**, 78 (1966)].
- ⁹G. T. Zatsepina, Author’s Abstract of Doctoral Dissertation (in Russian), Physics Institute of the USSR Academy of Sciences, M., 1954.
- ¹⁰A. E. Chudakov *et al.*, *Proceedings of International Conference on Cosmic Rays* (in Russian), USSR Academy of Sciences Press, M., 1960, Vol. 2, p. 47.
- ¹¹V. B. Atrashkevich *et al.*, *Proceedings of International Cosmic Ray Conference, La Jolla*, 1985, Vol. 7, p. 363.
- ¹²Yu. A. Fomin and G. B. Khristiansen, *Yad. Fiz.* **14**, 642 (1971) [*Sov. J. Nucl. Phys.* **14**, 360 (1972)].
- ¹³V. B. Atrashkevich, N. N. Kalmykov, and G. B. Khristiansen, *Pis’ma Zh. Eksp. Teor. Fiz.* **33**, 236 (1981) [*JETP Lett.* **33**, 225 (1981)].

Translated by M. E. Alferieff